Available online at www.sciencedirect.com

SciVerse ScienceDirect

Procedia Environmental Sciences 13 (2012) 935 – 942

Procedia Environmental Sciences

The 18th Biennial Conference of International Society for Ecological Modelling

Assess the effect of different degrees of urbanization on land surface temperature using remote sensing images

Z. Guo [a,*] , S.D. Wang[a], M.M. Cheng[c], Y. Shu[b]

[a] *State Key Laboratory of Earth Surface Processes and Resource Ecology, BeijingNormalUniversity, Beijng, 100875, China*

[b] *Academy of Disaster Reduction and Emergency Management Ministry of Civil Affairs & Ministry of Eduction, Beijing Normal University, Beijng, 100875, China*

[c] *International Institute for Earth System Science, Nanjing University, Nanjing, 210093, China*

Abstract

Urbanization is a human-dominated process and has greatly impacted biodiversity, ecosystem processes, and regional climate. In this study we assess the effect of different degrees of urbanization on land surface temperature using remote sensing images. Landsat TM images were used for land surface temperature retrieval using the algorithm proposed by Artis and Carnahan. ALOS multispectral images were used for landcover classification using classification trees in three study areas, namely Xicheng district(A), Haidian district(B)，Shijingshan district(C), of different degrees of urbanization in Beijing. Landcover-specific surface temperatures were estimated through an inversion alorithm. At the different degrees of urbanization, reducing the within-pixel coverage ratio of vegetations will result in an land surface temperature rise. Quantitative assessment of the relationship between different degrees of urbanization and land surface temperature was simulated by an urbanization index which integrates the coverage ratio of built-up landcover type and the cell-average NDVI. Urbanization indices of the Xicheng district, Haidian district, Shijingshan district were calculated to be 0.91, 0.72, and, 0.55 respectively. Such results are consistent with the trend of evaluation using quantitative estimation land surface temperature.

Keywords：Landcover; Urbanization; Land surface temperature.

1.Introduction

Studies of urbanization and urban thermal environment are now attracting wide interests among scientists all over the world.With rapid urbanization, there has been a tremendous growth in population and buildings in cities, which lead to the drastic reduction in the greenery area and oppositely the increase in impervious area. The core of the city becomes warmer than its periphery, thus forming an urban heat island—UHI[1]. Beijing, as our capital and one of the fastest economic development metropolitan in China, provides striking representation of such land conversion. This ongoing land change from natural surface to urban area definitely entails major ecological consequences that are yet to be fully studied[2, 3].Urban development can profoundly alter the urban landscape structures, and urban thermal environment. Timely and accurate information on the status and trends of urban ecosystems is critical to develop strategies for sustainable development and to improve urban residential environment and living quality[4, 5]. Thus,

* Corresponding author. Tel: +86+10+5880+7713

E-mail address: iamguozheng@yahoo.com.cn

1878-0296 © 2011 Published by Elsevier B.V. Selection and/or peer-review under responsibility of School of Environment, Beijing Normal University. Open access under CC BY-NC-ND license. doi:10.1016/j.proenv.2012.01.087

developing techniques and enhancing ability for monitoring urban expansion and urban thermal environment are greatly desired. Over the past few years, remotely sensed data of various spatial, spectral, angular, and resolutions have been widely used to study the Urban development, and to retrieve land surface biophysical parameters, such as vegetation abundances, built-up indices and land surface temperatures, that are good indicators of conditions of urban ecosystem[6]. The most apparent effect of urbanization is the increase of builtuplandcover. As the process of urbanization continues, the UHI areas expand and the coverage ratio of built-up landcover type increases. There exist a few definitions of urbanization index in the literature, including the ratio of apartment houses in total construction housing, road density and percentage of built area, and the ratio of building coverage per unit area[7]. These indices basically use the percentage of built area to quantify the degree of urbanization, and fail to consider the effect of vegetation cover. Thus, we use an urbanization index proposed by wei et al.[7]to analyze the degree of urbanization. These studies will definitely enrich our knowledge and understanding of urban ecological system and even our world.

2. Study areas and data pre-processing

The city of Beijing , the capital of China(39°54', 116°23')is located on north china plain with an area of 16,410km^2 and with a population of almost 18 million(2009).During the processes of rapid urbanization, this area, just like other metropolitan cities in the world, is experiencing tremendous pressure in terms of protection of eco-environment as well as management and operation of urban systems (Fig.1). Three regions (Xicheng district, Haidian district， Shijingshan district in Beijing) of different degrees of urbanization were chosen for this study. These regions include (1) a subregion centered at Xicheng district, (2) a subregion at Haidian district, and (3) a subregion at Shijingshan district. Xicheng district is a highly developed metropolitan and, in comparison, Haidian and Shijingshan are moderately developed urban areas. In fact, our study areas only encompasses some of the specialized zones in the resaerch areas.

Landsat TM images of September 2, 2009 was selected for use in this study based on the consideration of availability of good quality images (acquired under clear sky conditions). All images purchased were geometrically corrected and georeferenced to the WGS-84 datum and Universal TransverseMercator zone 50Ncoordinate system.In this study,we used the bands within solar reflectance spectral range to extract vegetation abundances, vegetation index, the band 6 (thermal infrared band) for each dataset was used to retrieve land surface temperatures. The raw digital numbers (DNs) were converted to radiances by applying the calibration coefficients (gains and offsets) specified in the Landsat handbook.

ALOS satellite multispectral images of these studies areas were collected. These images were acquired by the AVNIR2 sensor onboard the ALOS satellite with a spatial resolution of 10 m×10 m. Image acquisition dates of individual study areas is September 5, 2009. All these satellite images were preprocessed for radiometric and geometric corrections. Thus, all images were georeferenced to map projection coordinates.

Fig. 1. Location of study site (TM bands 7, 4, 3 for R, G, B).

3. Methods

3.1.Land surface temperature retrieval

For Landsat TM sensor, only one band located in the thermal infrared region, which is an important limitation in order to retrieve LST using widely used split-window method or temperature/emissivity separation algorithm and therefore to obtain the additional information about the emissivity is very necessary[8]. A variety of algorithms have been developed to retrieve land surface temperature from TM imagery, such as mono-window algorithm[9], single-channel algorithm[10] and the method proposed by Artis and Carnahan[11]. Besides emissivities, some extra parameters are required for using the mono-window algorithm and single-channel method, while the method developed by Artis and Carnahan[11] does not need extra input parameters and therefore was selected in this study. Please note that any one of these methods mentioned above was with the premise that the data was radiometric calibrated and the brightness temperatures were prior computed. The following equation was used to convert the digital number (DN) of Landsat5-TM TIR band to spectral radiance[12]:

$$L_\lambda = 0.0056322 * DN + 0.1238 \quad (1)$$

Then the following formula was used to convert the spectral radiance to at-sensor brightness temperature under the assumption of uniform emissivity[13]:

$$T_B = \frac{K_2}{\ln\left(\left(K_1 / L_\lambda\right) + 1\right)} \quad (2)$$

where T_B is the brightness temperature in Kelvin (K), L_λ is the spectral radiance in Wm-2 sr-1 mm-1; K_2 and K_1 are the prelaunch calibration constants, which are listed in Table 1.

To retrieve the land surface temperatures, the brightness temperatures obtained above must be scaled using emissivities of surface materials. A modified NDVI Threshold Method-NDVITHM recommended by Sobrino et al.[8] was used to produce the emissivity images for three dates with a modification of NDVI thresholds. Once the emissivity images were obtained, the LST can be derived according to:

$$LST = \frac{T_B}{1+(\lambda\sigma T_B/(hc))ln\varepsilon} \quad (3)$$

where λ is the effective wavelength (11.475 μ m for band 6 TM), σ is Boltzmann constant (1.38*10-23 J/K), h is Plank's constant (6.626*10-34 Js), c is velocity of light at a vacuum (2.998*108 m/s), ε is emissivity. The retrieved LST images were shown in Fig. 2.

3.2 Estimating the landcover-specific surface temperatures

Land surface temperatures derived from Landsat TM images represent average temperatures within a pixel which may be composed of several landcover types. Four major landcover types are present in the study area: (1) water ponds, (2) built-up areas (including paved roads, residential area, and factory buildings) and bare soils, (3) sparse vegetation, (4) vegetations. It is necessary to further estimate the apparent temperatures of individual landcover types from the land surface temperatures. This can be done by determining the coverage ratios of different landcover types within individual Landsat TM6 pixels using the multispectral ALOS images. Detailed procedures are described below.

Assume that k different landcover types are present in the study area. Within the spatial coverage of a pixel, each landcover type accounts for ω_i (i = 1, 2, . . . , k) coverage ratio of the total pixel coverage and the apparent temperatures of different landcover types are represented by T_i (i = 1, 2, . . . , k). The pixel-average land surface temperatures can thus be calculated as

$$\bar{T}(j) = \sum_{i=1}^{k} \omega_i(j) T_i(j), \qquad j = 1,2,\ldots,N \quad (4)$$

where j is the index specifying individual pixels in the LanddatTM6 images and N is the total number of pixels in the study area. The coverage ratios ω_i's not only vary with landcover types but also pixels.

We also assume that within the study area the apparent temperatures of specific landcover types do not vary with spatial locations, i.e.,

$$T_i(j) = T_i, \qquad j = 1,2,\ldots,N \quad (5)$$

where T_i's represent the landcover-specific apparent temperatures. Such assumption is reasonable since, for a specific landcover type, spatial variation of the apparent temperature within the study area (approximately 6000 m×6000 m) is

small, and more importantly the effect of landcover types on ambient air temperatures should be assessed on a region scale, not based on individual pixels. Thus, spatial variation of the pixelaverage land surface temperatures depends on coverage ratios of different landcover types present in individual Landsat TM6 pixels, i.e.,

$$\bar{T}(j) = \sum_{i=1}^{k} \omega_i(j) T_i, \qquad j = 1,2,\ldots,N \tag{6}$$

3.3 Assessing the degree of urbanization using an urbanization index

We propose to develop a cellspecific urbanization index by integrating the coverage ratio of built-up landcover type and the cell-average NDVI[7]:

$$\mathrm{UI_{cell}} = \mathrm{P_b}*(1\text{-}\mathrm{NDVI_{cell}}) \tag{7}$$

where $\mathbf{P_b}$ represents the coverage ratio of built-up landcover type of individual cells. Theoretically, the value of cell-specific urbanization index can vary between 0 and 2 since $-1 \leqslant \mathbf{NDVI_{cell}} \leqslant 1$. In reality, most $\mathbf{NDVI_{cell}}$ values fall in between 0 and 1, and higher $\mathbf{UI_{cell}}$ values indicate more significant effect of urbanization.

4. Results and analyses

4.1. Urban heat island effect

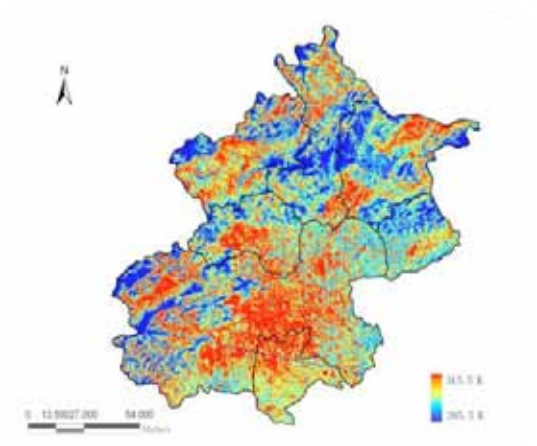

Fig. 2. LSTs derived from Landsat TM imagery.

In this study, the urban heat island was identified in the following way:

$$LST > \mu + 0.5 \mid \delta \text{ referred to UHI area} \tag{8}$$

$$0 < LST < \mu + 0.5 \mid \delta \text{ denoted non-UHI or rural area} \tag{9}$$

where μ and δ are the mean and standard deviation of temperatures in study area, respectively. The intensity of urban heat island was defined as the difference between average temperature of UHI area and that of rural area. The Results indicated that The spatial distribution of UHI was, to a large extent, in line with the pattern of built-up area. UHI area was mostly located at the places dominatedby high-rise and low-rise residential buildings, commercial areas,industrial areas and bare soils, which most of located in Beijing central city district,while the non-UHI area mainlyoccurred in water areas, high-and sparse-vegetation abundance areas, such as forests, crops or parks.

4.2. Effect of landcover types on land surface temperatures

Table 1. Estimated landcover-specific surface temperatures(K)

	W	B	S	V
A	300.46	300.97	299.97	299.91
B	299.98	300.09	299.82	299.38
C	299.52	300.85	299.94	296.71

W: water ponds, B: built-up, S: sparse vegetation, V: vegetations.

Table 1 indicates that surface temperatures vary with landcover types. Built-up areas with paved roads and residential and factory buildings have significant higher surface temperatures than other landcover types, while vegetation have the lowest surface temperatures. Although the built-up landcover has a significantly higher surface temperature than other landcover types, the different study area bult-up temperature differences are smaller. This is because the built-up landcover has the largest vertical temperature gradient.

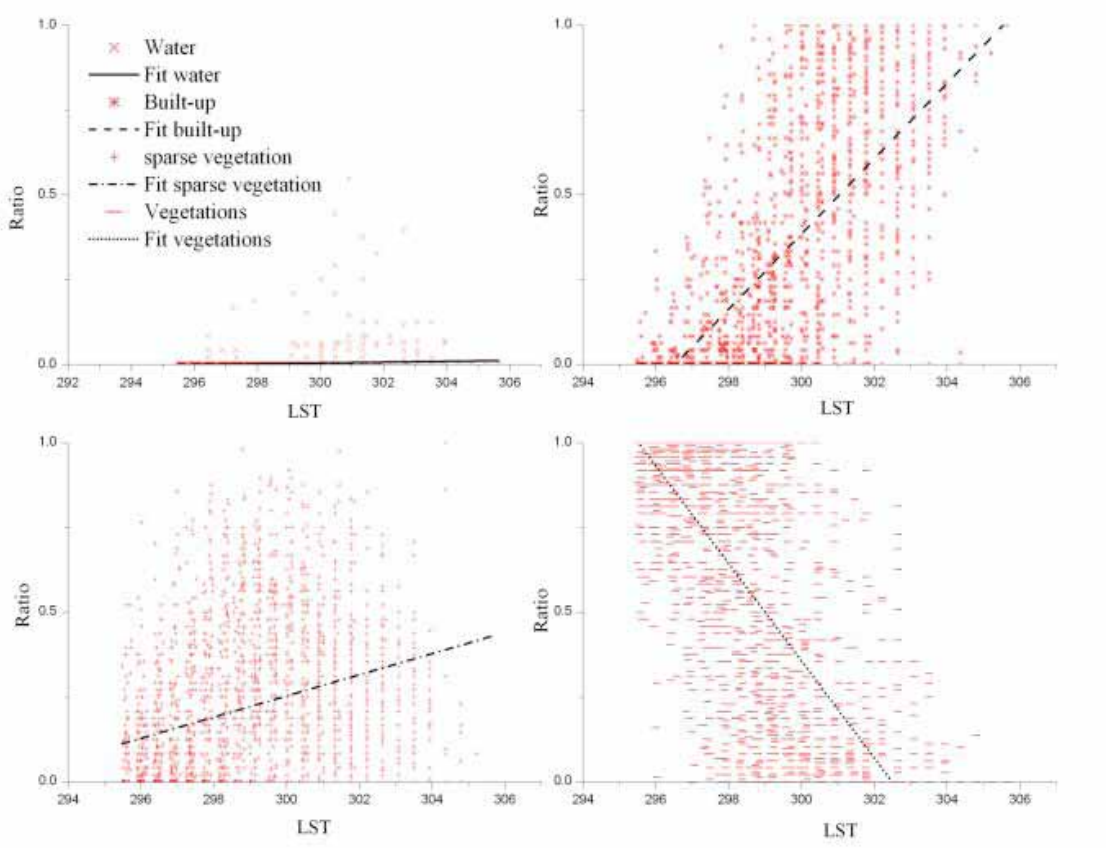

Fig.3. Empirical relationships between within-pixel coverage ratios of differentlandcover types and pixel-average temperatures.

Apart from comparing the landcover-specific air temperatures based on blind landcover conversions, another way of assessing the effect of landcover types on ambient air temperatures is by evaluating average surface temperatures with respect to coverage ratios of certain landcover types within individual Landsat TM6 pixels.

Fig.3. illustrates relationships between pixel-average LSTand within-pixel coverage ratios (CR) of different landcover types. All regression lines, particularly the one associated with the built-up landcover type, are very significant, suggesting well-established landcover patterns in the study area. It should be emphasized that, when the coverage ratios of built-up increased,theLST went up. Refering to the vegetations,theLST trend oppisite.

4.3. Relationships of LST to urbanization index

In previous studies, the relationships between temperature and vegetation were frequently investigated using the normalized difference vegetation index[14, 15] and most of them suggested that NDVI was strongly correlated to land surface temperature, however, the relationships of land surface temperature to vegetation abundance and percent impervious surface were not fully covered. Correlation analyses of the relationships between LSTs and other variables were further conducted at different scales: pixel- and regional-scale. Before applying the correlation analysis at pixel scale the pixel sizes of fraction and the LST images have to be rescaled to the same size[6]. However, this method must result in errors. Thus, we introduce the urbanization index produced by formula (7) to studying Relationships of LST to urbanization index.

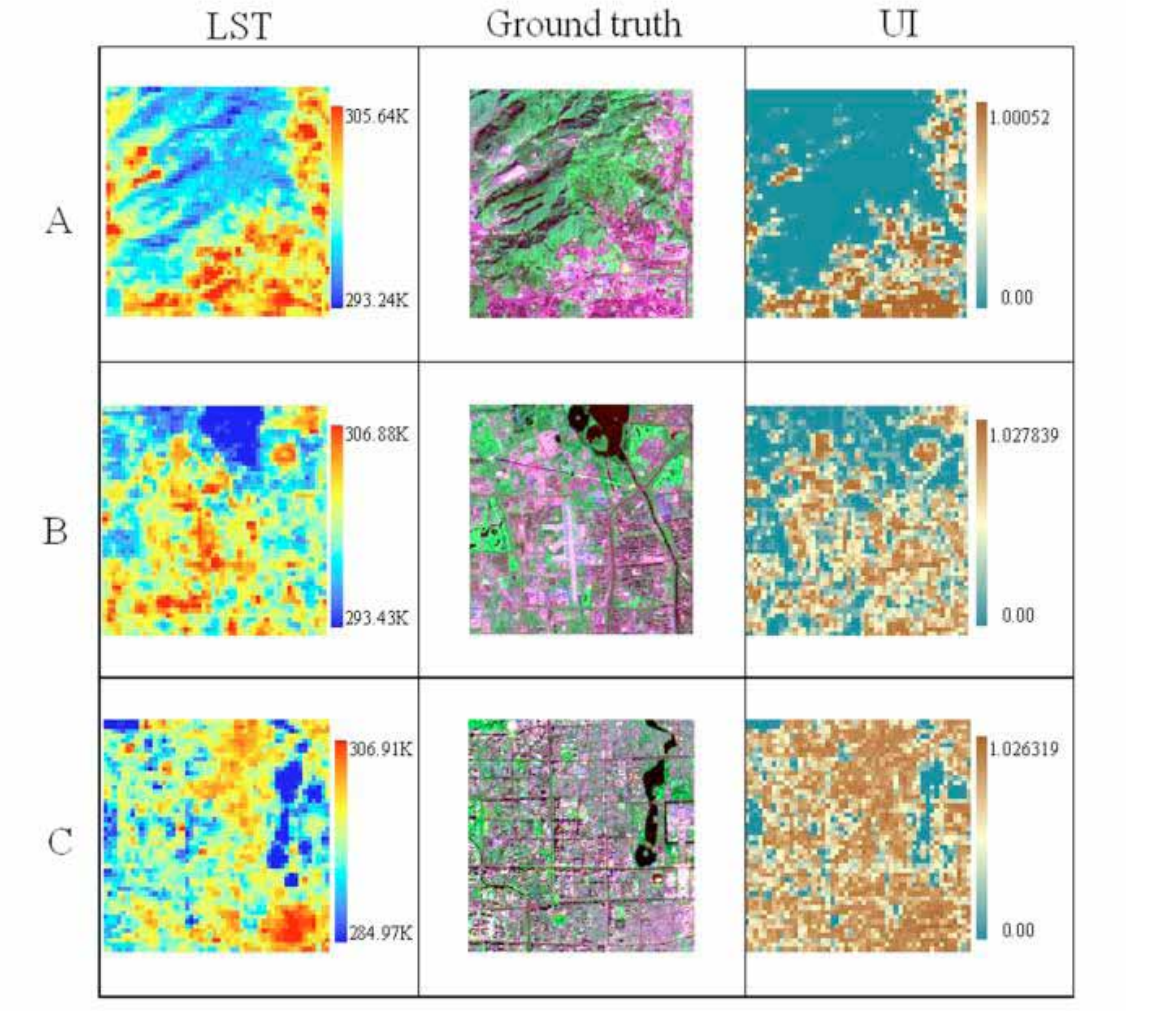

Fig. 4. LST derived from Landsat TM imagery, ground truth from ALOS, urbanization index derived from formula (7). A: subarea of Shijingshan, B: subarea of Haidian, C: subarea of Xicheng.

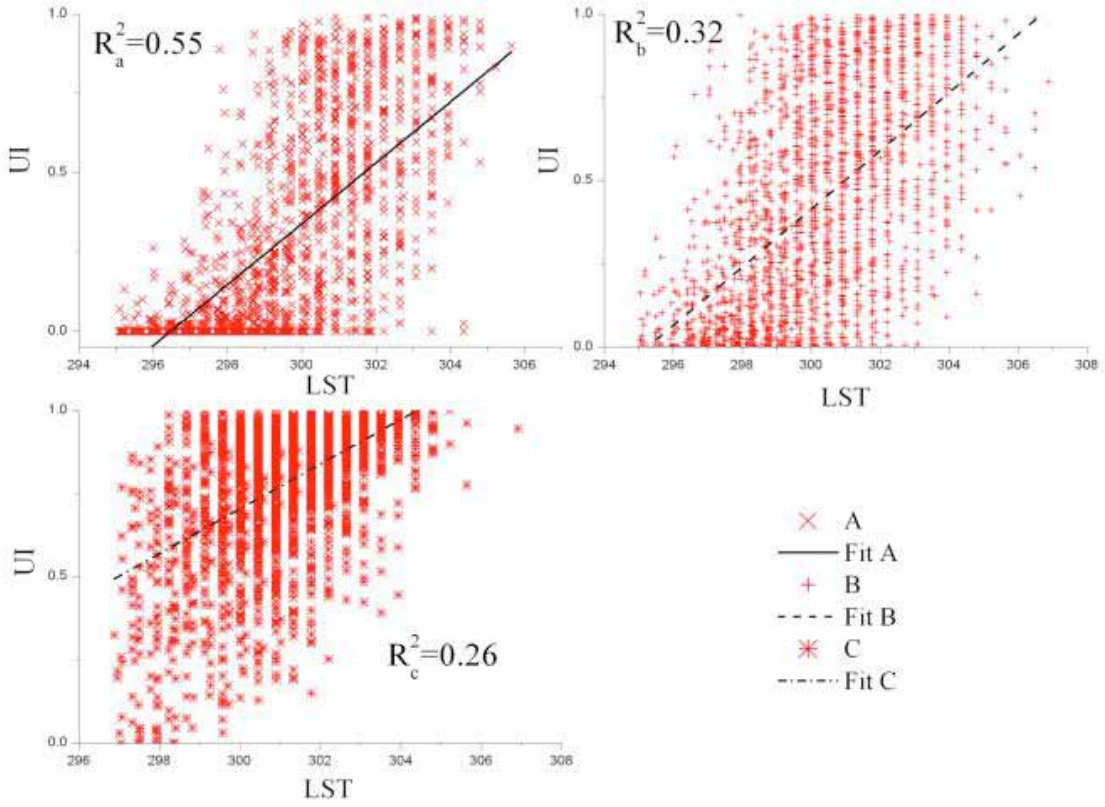

Fig. 5. Relationships of LST to UI

Land surface temperature and urbanization index of A,B,C were shown in Fig.4. C study area has the highest proportion of built-up dominated area, while A has the least. The areas with more diversified landcover seem to be located between areas with dominant landcover of built-up and vegetation, and maybe viewed as transition areas. The spatial pattern of different dominant landcover types in Fig. 4 not only is in good agreement with the UI, but also differentiates built-dominant and vegetation-dominant areas, affirming the feasibility of the LST. Quantitative assessment the relationship of LST to UI were also studied. The result were shown in Fig.5.

The coefficients of determination of LST to UI for three study areas were fairly low (maximum R-squarevalue was less than 0.6), and the same situation was found in relationships of LST to NDVI. These results implied that at cell-scale, the relationships of LST to UI could not be simply expressed using the linear model, there might be more complicated unknown associations between them, which need to be further studied in future research. However, we also could get a result that the LST increased when urbanization degree went up.

5. Discussion and conclusions

In this paper, Landsat TM and ALOS images were used to investigate the influences of urbanization on urban thermal environment and to examine the relationships of thermal characteristics to urbanization index in Beijing. Comparison analyses between landcover-specific surface temperature and different landcover ratio, comparison analyses between LST to UI at cell scale were sequentially conducted. The urbanization analyses showed that Beijing experienced a rapid urbanization, the degree of different urbanization in different were 0.91, 0.72, and, 0.55.

Comparison analyses of the relationships of LST to UI indicated that at the cell-scale, the relationships of LST to UI was relatively more complicated. The relationship was notvery positive. This can be probably attributed to: (1) the variations of the LST was highly suppressed by zonal computing and (2) the influence of sampling manner on the correlation was greatly reduced at cell-scale.

Further works are needed to: (1) quantitatively validate the new enhancing method employed to map impervious surface using finer spatial resolution images. (2) The urbanization index was a 2D parameter, when analyze the relationship between LST and UI,may be we should consider the elevation. We can introduce DEM as aparameter consist of the UI. In addition, studies of other metropolitans and different remotely sensed data are also recommended.

Acknowledgments

This work is jointly funded by project (No. 2010DFA32920) from State Key Laboratory of Earth Surface Processes and Resource Ecology, Beijing Normal University. We are indebted to Wang shidong for their assistance in improving the readability of this manuscript. The authors also want to gratefully acknowledge two classmates providing me with their constructional comments and suggestions.

References

[1].Voogt, J. and T. Oke, Thermal remote sensing of urban climates.*Remote Sensing of Environment*, 2003. **86**(3): 370-84.

[2].Wu, J. and J.L. David, A spatially explicit hierarchical approach to modeling complex ecological systems: theory and applications.*Ecological Modelling*, 2002. **153**(1-2): 7-26.

[3].Grimm, N.B. and C.L. Redman, Approaches to the study of urban ecosystems: the case of Central Arizona¡ªPhoenix.*Urban Ecosystems*, 2004. **7**(3): 199-213.

[4].Song, C., Spectral mixture analysis for subpixel vegetation fractions in the urban environment: How to incorporate endmember variability? *Remote Sensing of Environment*, 2005. **95**(2): 248-63.

[5].Yang, L., et al., Urban land-cover change detection through sub-pixel imperviousness mapping using remotely sensed data.*Photogrammetric engineering and remote sensing*, 2003. **69**(9): 1003-10.

[6].Ma, Y., Y. Kuang, and N. Huang, Coupling urbanization analyses for studying urban thermal environment and its interplay with biophysical parameters based on TM/ETM+ imagery.*International Journal of Applied Earth Observation and Geoinformation*, 2010. **12**(2): 110-18.

[7].Hung, W.C., Y.C. Chen, and K.S. Cheng, Comparing landcover patterns in Tokyo, Kyoto, and Taipei using ALOS multispectral images.*Landscape and Urban Planning*, 2010. **97**(2): 132-45.

[8].Sobrino, J., Land surface temperature retrieval from LANDSAT TM 5.*Remote Sensing of Environment*, 2004. **90**(4): 434-40.

[9].Qin, Z., A. Karnieli, and P. Berliner, A mono-window algorithm for retrieving land surface temperature from Landsat TM data and its application to the Israel-Egypt border region.*International Journal of Remote Sensing*, 2001. **22**(18): 3719-46.

[10].Jim¨¦nez-Mu oz, J.C. and J.A. Sobrino, A generalized single-channel method for retrieving land surface temperature from remote sensing data.*Journal of geophysical research*, 2003. **108**(D22): 4688-95.

[11].Artis, D.A. and W.H. Carnahan, Survey of emissivity variability in thermography of urban areas.*Remote Sensing of Environment*, 1982. **12**(4): 313-29.

[12].Markham, B.L. and J.L. Barker, Spectral characterization of the Landsat Thematic Mapper sensors.*International Journal of Remote Sensing*, 1985. **6**(5): 697-716.

[13].Wukelic, G., et al., Radiometric calibration of Landsat Thematic Mapper thermal band.*Remote Sensing of Environment*, 1989. **28**: 339-347.

[14].Owen, T., T. Carlson, and R. Gillies, An assessment of satellite remotely-sensed land cover parameters in quantitatively describing the climatic effect of urbanization.*International Journal of Remote Sensing*, 1998. **19**(9): 1663-81.

[15].Yuan, F. and M.E. Bauer, Comparison of impervious surface area and normalized difference vegetation index as indicators of surface urban heat island effects in Landsat imagery.*Remote Sensing of Environment*, 2007. **106**(3): 375-86.